© 2021. Published by The Company of Biologists Ltd | Journal of Cell Science (2021) 134, jcs252320. doi:10.1242/jcs.252320

RESEARCH ARTICLE

SPECIAL ISSUE: CELL BIOLOGY OF HOST–PATHOGEN INTERACTIONS

FIB-SEM-based analysis of *Borrelia* intracellular processing by human macrophages

Matthias Klose[1], Maximilian Scheungrab[2], Manja Luckner[2], Gerhard Wanner[2,*] and Stefan Linder[1,*]

ABSTRACT

Borrelia burgdorferi is the causative agent of Lyme disease, a multisystemic disorder affecting primarily skin, joints and nervous system. Successful internalization and intracellular processing of borreliae by immune cells, like macrophages, is decisive for the outcome of a respective infection. Here, we use, for the first time, focused ion beam scanning electron microscopy tomography (FIB-SEM tomography) to visualize the interaction of borreliae with primary human macrophages with high resolution. We report that interaction between macrophages and the elongated and highly motile borreliae can lead to formation of membrane tunnels that extend deeper into the host cytoplasm than the actual phagosome, most probably as a result of partial extrication of captured borreliae. We also show that membrane tubulation at borreliae-containing phagosomes, a process suggested earlier as a mechanism leading to phagosome compaction but hard to visualize in live-cell imaging, is apparently a frequent phenomenon. Finally, we demonstrate that the endoplasmic reticulum (ER) forms multiple STIM1-positive contact sites with both membrane tunnels and phagosome tubulations, confirming the important role of the ER during uptake and intracellular processing of borreliae.

This article has an associated First Person interview with the first author of the paper.

KEY WORDS: *Borrelia*, FIB-SEM tomography, Macrophage, Membrane tubulation, Phagosome, STIM1

INTRODUCTION

Borrelia burgdorferi is a spirochetal bacterium characterized by an elongated helical shape (Li et al., 2000) and a length of up to 40 µm (Aberer and Duray, 1991). Borreliae are highly motile and can reach velocities of up to 4 µm/s (Moriarty et al., 2008), which is based on the presence of periplasmic flagella that run along the entire length of the spirochete (Goldstein et al., 1994; Li et al., 2000), driven by a cytoplasmic ATPase complex (Qin et al., 2018).

Borreliae propagate in small animals, such as rodents, deer or birds, but can also be transferred to a human host via a tick bite (Lane and Loye, 1991), with a resulting infection potentially causing Lyme disease, a multisystemic disorder that affects mainly skin, joints and the nervous system. A frequent initial sign of a borreliae infection is the development of *erythema migrans*, a skin rash that spreads in the form of a bull's eye from the site of infection. This rash is enriched in immune cells such as macrophages, dendritic cells and neutrophils (Salazar et al., 2003), cells that represent the first line of the human immune defense. Successful capturing of borreliae by immune cells, with subsequent phagocytic uptake and intracellular processing in phagolysosomes is thus decisive for the outcome of a respective infection.

Immune cells such as macrophages are able to recognize borreliae through several receptors (Carreras-Gonzalez et al., 2019), including FcγR (Benach et al., 1984; Montgomery et al., 1994) and complement receptor 3 (CR3) (Cinco et al., 1997; Hawley et al., 2012). Immobilization of the highly motile spirochetes at the host cell surface is achieved by filopodia, cell protrusions rich in linear actin filaments (Svitkina et al., 2003) that are regulated by formins such as FMNL1, mDia1 (Naj et al., 2013) and Daam1 (Hoffmann et al., 2014). Further enwrapping of spirochetes proceeds through formation of an F-actin-rich coiling pseudopod (Rittig et al., 1992), regulated by Daam1 (Hoffmann et al., 2014) and also by the Arp2/3 complex (Linder et al., 2001).

Owing to the pronounced length of the spirochete, partial internalization of borreliae is frequent, with parts of the captured *Borrelia* cell still being extracellular (Rittig et al., 1994). Internalization of captured borreliae proceeds via uptake into phagosomes that are enriched in the RabGTPase Rab22a at their surface (Naj and Linder, 2015). Furthermore, borreliae-containing phagosomes are contacted by vesicles positive for Rab5a that are in close contact to the endoplasmic reticulum (ER) (Naj and Linder, 2015). Accordingly, the ER-coordinated activities of Rab22a and Rab5a have been proposed to lead to the formation and detachment of membrane tubules at the site of vesicle–phagosome contact, resulting in the reduction of the phagosomal surface and thus in the compaction of phagosome-packaged spirochetes (Naj and Linder, 2015, 2017). Membrane tubulation is important for further phagolysosomal maturation and eventual clearance of spirochetes from immune cells. In consequence, siRNA-mediated depletion of members of the Rab22a-SNX3-Rab5a pathway, either singly or in combination, leads to defects in compaction of phagosomes, accompanied by reduced proteolytic capacity of phagosomes and enhanced intracellular survival of spirochetes (Klose et al., 2019; Naj and Linder, 2015). However, phagosomal membrane tubulation is hard to visualize by conventional microscopic techniques, such as live-cell imaging, raising questions about the frequency of this phenomenon.

In order to test and extend our previous findings on borreliae processing by macrophages, we resorted to ultrastructural analysis of samples of macrophages with internalized borreliae. We now report, for the first time, the use of focused ion beam scanning electron microscopy tomography (FIB-SEM tomography) for analysis of the interaction of borreliae with immune cells in unprecedented detail. So far, ultrastructural analyses using techniques such as SEM or cryo-transmission electron microscopy (TEM) have been mostly limited to the investigation of the spirochetes themselves (Kudryashev et al., 2011; Lemgruber et al., 2015; Vancová et al., 2017), and in particular to the analysis of

[1]Institute for Medical Microbiology, Virology and Hygiene, University Medical Center Eppendorf, 20246 Hamburg, Germany. [2]Biozentrum der Ludwig-Maximilians-Universität, 82152 Planegg-Martinsried, Germany.

*Authors for correspondence (wanner@lrz.uni-muenchen.de; s.linder@uke.de)

M.K., 0000-0002-6206-5307; M.S., 0000-0003-2736-7681; M.L., 0000-0002-9915-2842; G.W., 0000-0002-5996-5902; S.L., 0000-0001-8226-2802

Handling Editor: Derek Walsh
Received 29 July 2020; Accepted 15 December 2020

Journal of Cell Science (2021) 134, jcs252320. doi:10.1242/jcs.252320

their flagellar motor complex (Chang et al., 2019; Liu et al., 2009; Xu et al., 2011), while interaction of spirochetes with human tissues or immune cells has been analyzed mainly by using conventional EM techniques (Duray et al., 2005; Rittig et al., 1994).

In the current study, we established a correlative light-electron microscopy (CLEM)-based technique using FIB-SEM microscopy to embed samples of macrophages infected with borreliae on slides with a laser-marked coordinate system within an ultra-thin resin layer. Use of this technique allows for rapid and precise correlation to light microscopy micrographs and also for FIB milling in any desired direction. These advantages enable precise alignments of slides within a FIB stack and thus subsequent volume rendering for direct 3D visualization at high resolution. We report that membrane tubulation at phagosomes is indeed a frequent phenomenon occurring at borreliae-containing phagosomes. We also confirm that the ER forms multiple sites of close contact with nascent and compacted phagosomes, further underlining its importance for internalization and intracellular processing of spirochetes. Moreover, we find that membrane tunnels, a novel phagocytic structure, extend farther into the host cell cytoplasm than the actual phagosomes, which may be based on partial extrication of the highly mobile borreliae from host cells, indicating that the uptake process of borreliae by immune cells is likely more complex than previously assumed.

RESULTS

Work flow – from cell seeding to 3D rendering

For preparation of specimens of macrophages interacting with *Borrelia* spirochetes for FIB-SEM microscopy, primary human macrophages were seeded on glass slides with a laser-marked grid, which allows later alignment of light and scanning electron microscopy (SEM) images. Cells were infected with GFP-expressing borreliae at a multiplicity of infection (MOI) of 30:1, and specimens were fixed after 1 h of incubation, and stained for DNA using DAPI. Cells for analysis were selected by correlative light- and electron microscopy (CLEM). In a first step, light microscopy was used to detect target cells based on the presence of both DAPI and borreliae-based GFP signals (Fig. 1A,B). Following ultrathin embedding in resin, target cells were then re-localized using SEM (Fig. 1C–F). DAPI and GFP fluorescence signals were superimposed on SEM specimens, allowing precise definition of regions of interest for focused ion beam (FIB) milling (Fig. 1E,F).

Of note, ultrathin embedding of specimens allowed direct milling of target regions of interest, without the usual need of milling a ramp to gain access to these sites of the specimen. Regions of interest were then subjected to alternating FIB milling of sections of 20 nm thickness, followed by SEM-based recording of respective images (Fig. 1G). Image stacks of whole macrophages were thus recorded by generating stacks of 2000–3000 images within 10–15 h, allowing the reconstruction of whole cells or defined regions of interest in high resolution (Movie 1). Image stacks were subsequently segmented and reconstructed using Amira™ software and false color-coding to visualize respective cellular compartments and internalized borreliae (Movie 1).

Phagocytosis of borreliae can induce membrane tunnels in the macrophage cytoplasm

Confirming earlier reports (Linder et al., 2001; Rittig et al., 1992), borreliae in contact with macrophages were often found to be at

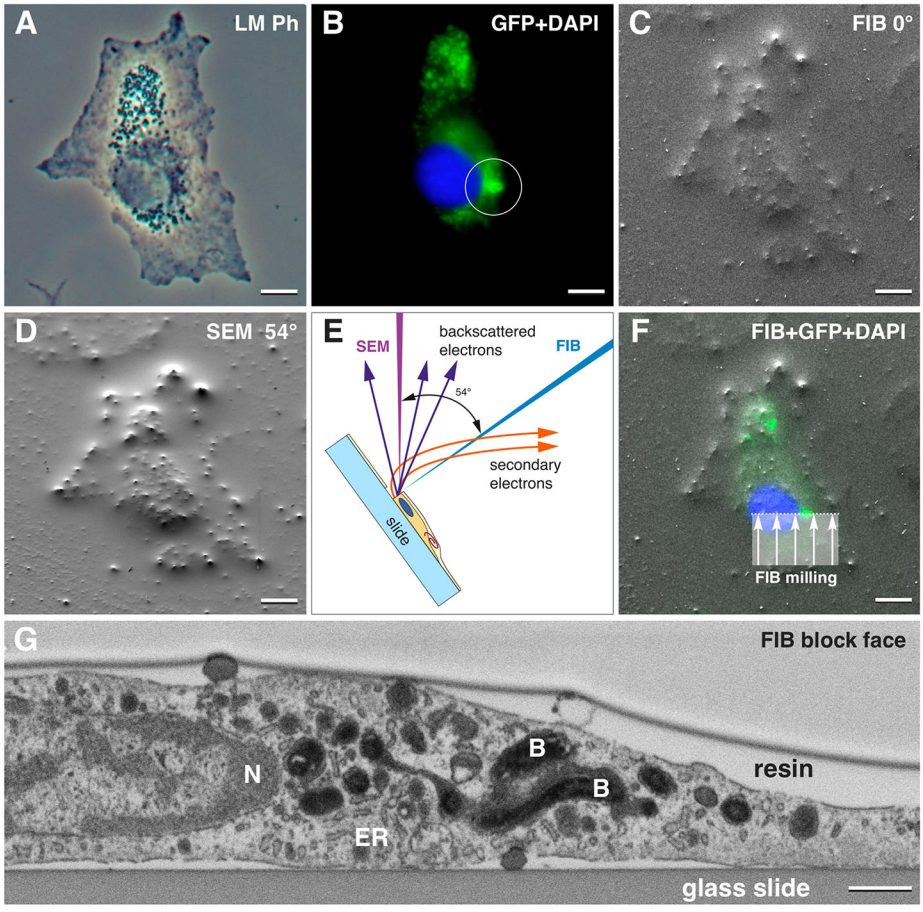

Fig. 1. Work flow of correlative light and FIB-SEM electron microscopy of macrophages infected with borreliae. (A) Bright-field phase-contrast micrograph (LM Ph) of human macrophage seeded on laser-marked slide and incubated with GFP-expressing borreliae. (B) Fluorescence micrograph of cell shown in A. GFP and DAPI signals show *Borrelia* cells in contact with a macrophage and location of the nucleus for CLEM. (D,E) After fixation and ultrathin embedding in resin, target cells are re-localized in SEM by the electron beam. The specimen is tilted to the coincidence point (54°) to allow perpendicular milling of the sample by the ion beam. Corresponding SEM and FIB images are indicated. (F) After superposition of the fluorescence signals, FIB milling can be defined with high precision. Site of FIB milling is indicated by field of white arrows. (G) A stack of micrographs is taken from the block face using the back scattered electron signal; a representative slice is shown; B, *Borrelia* cell; N, nucleus. Scale bars: 10 µm (A–F), 1 µm (G).

Journal of Cell Science (2021) 134, jcs252320. doi:10.1242/jcs.252320

least partially enwrapped by multiple membrane folds containing cytoplasm, leading to the formation of coiling pseudopods (Fig. 2; Fig. S1, Movie 2). Further rendering of the macrophage surface showed that captured borreliae were enwrapped not only by a single coiling pseudopod, but by multiple elaborate membrane folds that arose from the macrophage surface and apparently immobilized the captured spirochete in several places along its length (Fig. 2A; Movie 3). Further visualization of the host cell membranes associated with uptake of borreliae showed that the internalized parts of spirochetes were surrounded by a membranous compartment within the host cytoplasm, most probably representing the nascent phagosome (Fig. 2B), as previously described (Naj and Linder, 2015). Surprisingly, however, further rendering showed that these phagocytosis-associated membranes were not always closely following the morphology of the spirochete, but could also extend more than 10 µm further into the host cytoplasm than the most distal part of the internalized borreliae (Fig. 2B,C; Movie 3; see also Fig. 6A).

Based on their morphology, we termed these longer membrane extensions into the host cytoplasm 'tunnels'. It could be envisioned that membrane tunnels are formed as a result of partial extrication of the highly motile borreliae, thus representing sites of former phagosomes. This assumption seems to be supported by the observation that the ER forms multiple sites of contact with membrane tunnels (Fig. 3A–D; Movie 4), as also previously described for nascent borreliae-containing phagosomes (Naj and Linder, 2015). ER contact sites thus seem to be retained at the tunnels, even after partial relocalization of the *Borrelia* cell within the phagosome–tunnel complex.

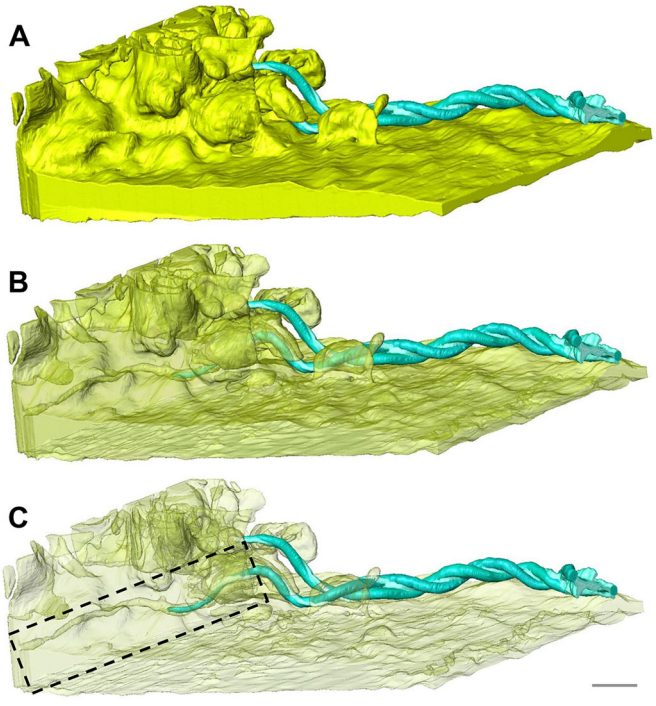

Fig. 2. Rendering of macrophage surfaces reveals *Borrelia*-associated membrane tunnels. *Borrelia* (turquoise), with endoflagella (light blue), coiled upon itself, with both ends embedded in multiple membrane folds of the macrophage surface (yellow). Images 1–3 have increasing transparency. Dashed-black box indicates part of the *Borrelia* cell with associated membrane tunnel, visualized in Fig. 3. Scale bar: 1 µm.

Borrelia-associated phagosomes and tunnels are positive for phosphatidylserine

In order to test whether membrane tunnels detected by FIB-SEM could also be observed by confocal microscopy, we visualized borreliae-containing phagosomes in macrophages expressing GFP–Rab22a, which is enriched at *Borrelia*-containing phagosomes (Naj and Linder, 2015). However, as GFP–Rab22a shows low transfection efficiency in primary macrophages, and tunnels are only formed in a subset of phagocytic events, we also tested alternative markers for borreliae phagosomes, which showed better transfection efficiencies. One such marker is RFP–LactC2, a construct containing the C2 domain of lactadherin and acting as a reporter of phosphatidylserine (Kay and Grinstein, 2011; Yeung et al., 2008), which is ubiquitously present at the inner leaflet of the plasma membrane and, as the phagosomal membrane is directly derived from invagination of the plasma membrane, also on the outside of early phagosomes (Maxson and Grinstein, 2020). Coexpression of RFP–LactC2 together with GFP–Rab22a in macrophages showed that, upon phagocytic uptake of borreliae, GFP–Rab22a and also RFP–LactC2, were both recruited to nascent phagosomes (Fig. 4A–D), with RFP–LactC2 even marking parts of phagocytosed borreliae that were not positive for GFP–Rab22a (Fig. 4A1–D1). In the following sections, RFP–LactC2 was thus used as a marker for borreliae phagosomes.

To visualize borreliae phagosome-associated membrane tunnels, GFP-expressing borreliae were incubated for 30 min with primary human macrophages expressing RFP–LactC2, with subsequent fixing of samples without permeabilization, and staining of extracellular parts of borreliae using a *Borrelia*-specific antibody. As expected, internalized parts of borreliae were found to be enwrapped by RFP–LactC2-positive membranes (Fig. 4E,F). Vice versa, parts of spirochetes not enwrapped by RFP–LactC2-positive membranes were extracellular, as determined by an outside staining technique (Fig. 4E–H). Importantly, at borreliae that were not fully internalized, the RFP–LactC2 signal occasionally extended further into the cytoplasm than the actual spirochete (Fig. 4E1–H1), pointing to the existence of membrane tunnels, as detected previously by FIB-SEM. Membrane tunnels were detected at 2–5% of all partially internalized borreliae. Quantification of tunnel lengths, based on respective RFP–LactC2 signals, showed that tunnels can extend up to 10 µm into the cytoplasm, with the majority of tunnels falling into the 2–6 µm size range (Fig. 4I). Tunnel-associated borreliae had a mean±s.e.m. length of 17.2±1.2 µm, with the larger part of the spirochete body being extracellular (13.9±1.6 µm), and only a minor part being intracellular (3.3±1.1 µm). Associated tunnels showed a mean length of 4.9±0.6 µm.

Borreliae phagosomes have restricted access to the extracellular space

Interestingly, use of the outside staining technique also showed that accessibility of the *Borrelia*-specific antibody was not necessarily restricted to the extracellular parts of spirochetes, which were not enwrapped in a phagosomal membrane and thus free of a RFP–LactC2 signal. In addition, we also observed that proximal parts of borreliae-containing phagosomes were often accessible for antibody staining (Fig. 5A). Respective antibody-based signals were strongest at the phagosome entry site and gradually decreased towards the distal parts of phagosomes (Fig. 5A1–A4,A1′–A4′,B).

Further analysis of respective immunofluorescence images showed that the RFP–LactC2-positive membrane from

Journal of Cell Science (2021) 134, jcs252320. doi:10.1242/jcs.252320

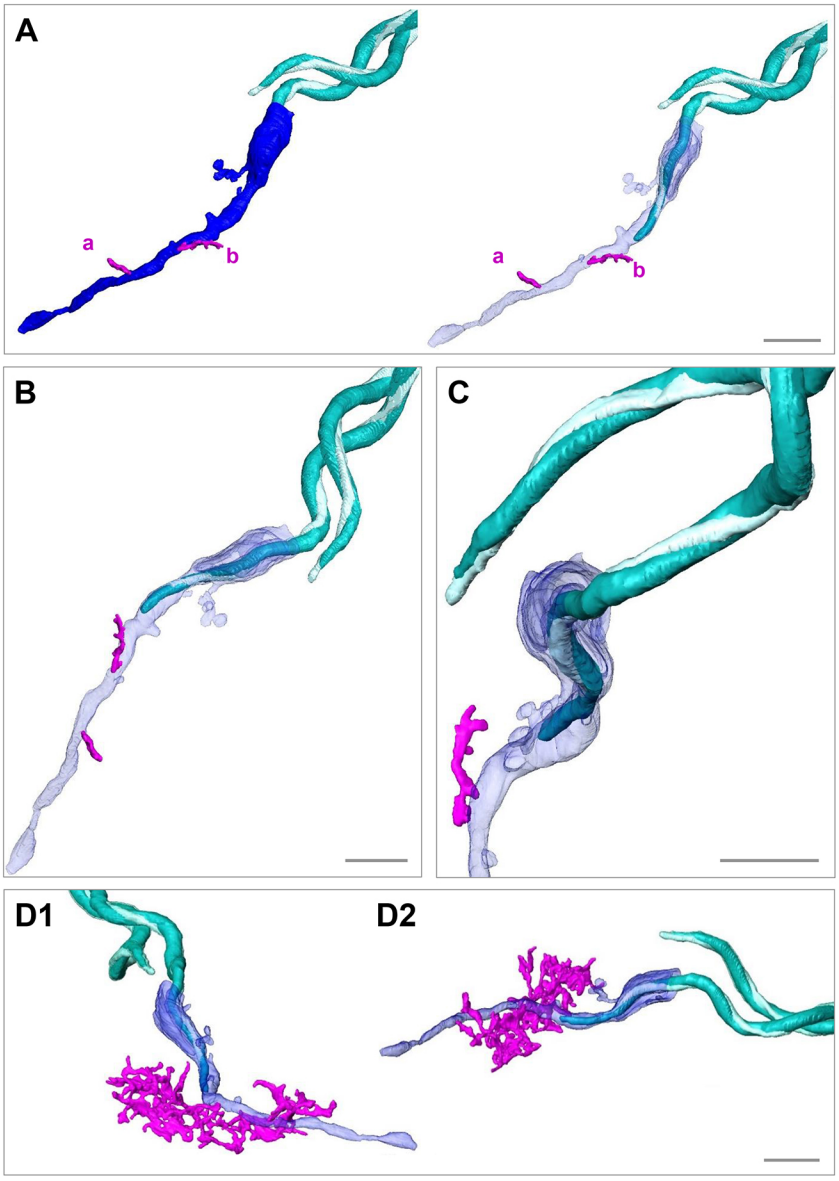

Fig. 3. The ER is in contact with *Borrelia*-associated membrane tunnels. (A–D) FIB-SEM-based renderings of captured *Borrelia* cell shown in Fig. 2, with associated membrane structures of the host cell. (A) Left, surface of phagosome and membrane tunnel in dark blue. Right, increased transparency. Attachment sites of the ER (a,b) are in magenta. (B,C) Different perspectives of the structures shown in A. (D1,D2) Further rendering of associated ER, in two different perspectives. Scale bars: 1 µm.

incompletely closed phagosomes often followed the outline of borreliae only loosely, resulting in infrequent points of close contact between internalized spirochetes and phagosomal membrane (Fig. 5A1′–A4′). This was further corroborated by use of the SurfaceIntersect tool of Amira™ software, to re-analyze the FIB-SEM-generated image stacks, which showed that sites of close contact between borreliae and phagosomes were present as isolated patches along the whole length of internalized spirochetes (Fig. 5C). Collectively, these findings indicate that incompletely closed borreliae phagosomes gradually accumulate isolated contact sites along their inner length and are not sealed off completely from the extracellular space. This seems also to be in line with the observed partial accessibility for antibodies to the proximal parts of *Borrelia*-containing phagosomes.

Compaction of phagosomes is associated with membrane tubulation

Phagosomes containing borreliae internalized by macrophages are compacted from an initial elongated morphology, following the outline of spirochetes, to a closely packed spherical form, which is a prerequisite for further phagolysosomal maturation (Klose et al., 2019; Naj and Linder, 2015, 2017). Compaction of phagosomes has been proposed to proceed via extrusion of membrane tubules from phagosomes, thus leading to a progressive reduction of the phagosome surface (Naj and Linder, 2015). However, this process takes place within a time frame of minutes and also in multiple optical planes and is thus hard to visualize by conventional microscopic methods such as live-cell imaging.

Therefore, we visualized borreliae-containing phagosomes using FIB-SEM tomography and 3D rendering at various stages of compaction. Indeed, we observed that phagosomes containing still elongated spirochetes already form membrane tubules, and especially at sites of curvature discontinuities, for example, when the phagosomal membrane is in close contact with helical bends of the internalized spirochetes or at the distal end of respective phagosomes (Fig. 6A). Moreover, even within a single macrophage containing several borreliae phagosomes in various stages of compaction, multiple events of membrane tubulation

Journal of Cell Science (2021) 134, jcs252320. doi:10.1242/jcs.252320

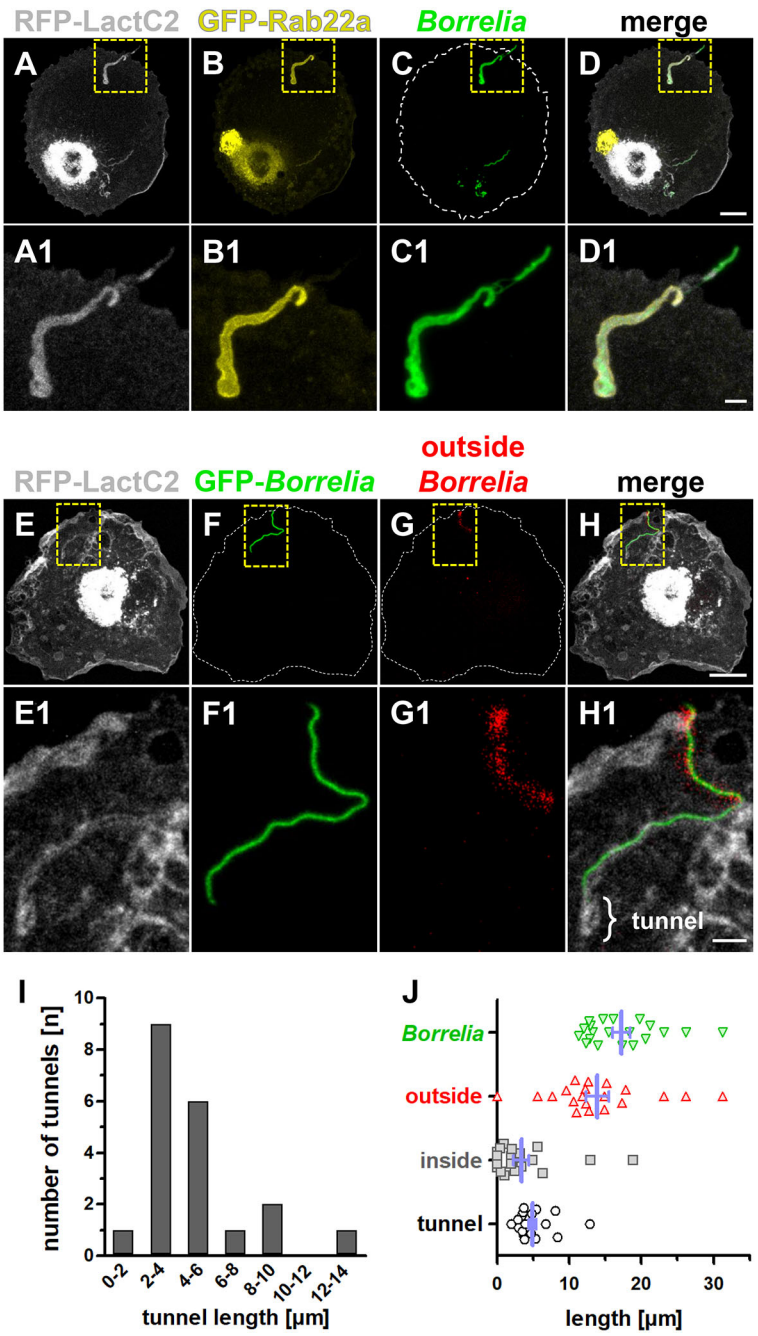

Fig. 4. *Borrelia*-associated phagosomes and tunnels are positive for phosphatidylserine. (A–D) Immunofluorescence micrographs of primary macrophage expressing RFP–LactC2, a reporter for phosphatidylserine (white) (A), and phagosome marker GFP–Rab22a (yellow) (B), with partially internalized GFP-expressing *Borrelia* cells (green) (C), with merge (D). Dashed-yellow boxes in overview images indicate region shown enlarged in detail images (A1–D1). (E–H) Immunofluorescence micrographs of primary macrophage expressing RFP–LactC2, (white) (E), with partially internalized GFP-expressing *Borrelia* cells (green) (F), stained by outside staining technique using *Borrelia*-specific antibody for extracellular parts of the spirochete (red) (G), with merge (H). Dashed-yellow boxes in overview images indicate region shown enlarged in detail images (E1–H1). *Borrelia*-free membrane tunnel is indicated by bracket. Scale bars: 10 µm for overviews, 2 µm for detail images. (I,J) Quantification of tunnel length. A total of 20 tunnels from 18 cells are plotted according to their relative lengths in µm, with bar diagram showing tunnels grouped into respective categories. (J) Individual occurrences of tunnels are characterized by the respective length of tunnel-associated borreliae (‘*Borrelia*’), of their extracellular (‘outside’) and intracellular (‘inside’) parts, as determined by inside-outside staining, and of associated tunnels (‘tunnel’), as determined by associated RFP–LactC2 signals (n=20, from 6 different donors). The mean±s.e.m. is also shown.

could be observed, and especially at incompletely compacted phagosomes (Fig. 6B–B2,C–C2; Movies 4–6). We conclude that membrane tubulation at borreliae-containing phagosomes is indeed a frequent phenomenon that is closely associated with phagosomal compaction and likely also causative for this phenomenon.

The ER forms multiple contact sites with tunnels and phagosomes

In earlier studies, we observed a close proximity between borreliae-containing phagosomes and the ER (Naj and Linder, 2015). We therefore also proceeded to render the ER around the diverse structures associated with uptake of borreliae. We could confirm that the ER closely associates with all borreliae-containing structures, including membrane tunnels, nascent incompletely closed phagosomes and also phagosomes undergoing compaction. Indeed, ER was found to form several sites of attachment to these structures. In the case of membrane tunnels (Fig. 3A–D2; Movie 4), this probably reflects the ER being retained at contact sites from prior phagosomes, as mentioned above. In the case of phagosomes (Fig. 6; Movies 4–6), ER contacts could serve as anchoring points for ER-associated vesicles, which have been shown to dock at phagosomes through the vesicle component SNX3 binding the phosphoinositide PI(3)P within the phagosomal coat (Klose et al., 2019).

Further rendering of ER–phagosome contacts at higher magnification showed that parts of the ER showed distinct sites of close contact with associated phagosomes, indicating that these structures might be not simply due to fortuitous closeness (Fig. 7A,B;

Journal of Cell Science (2021) 134, jcs252320. doi:10.1242/jcs.252320

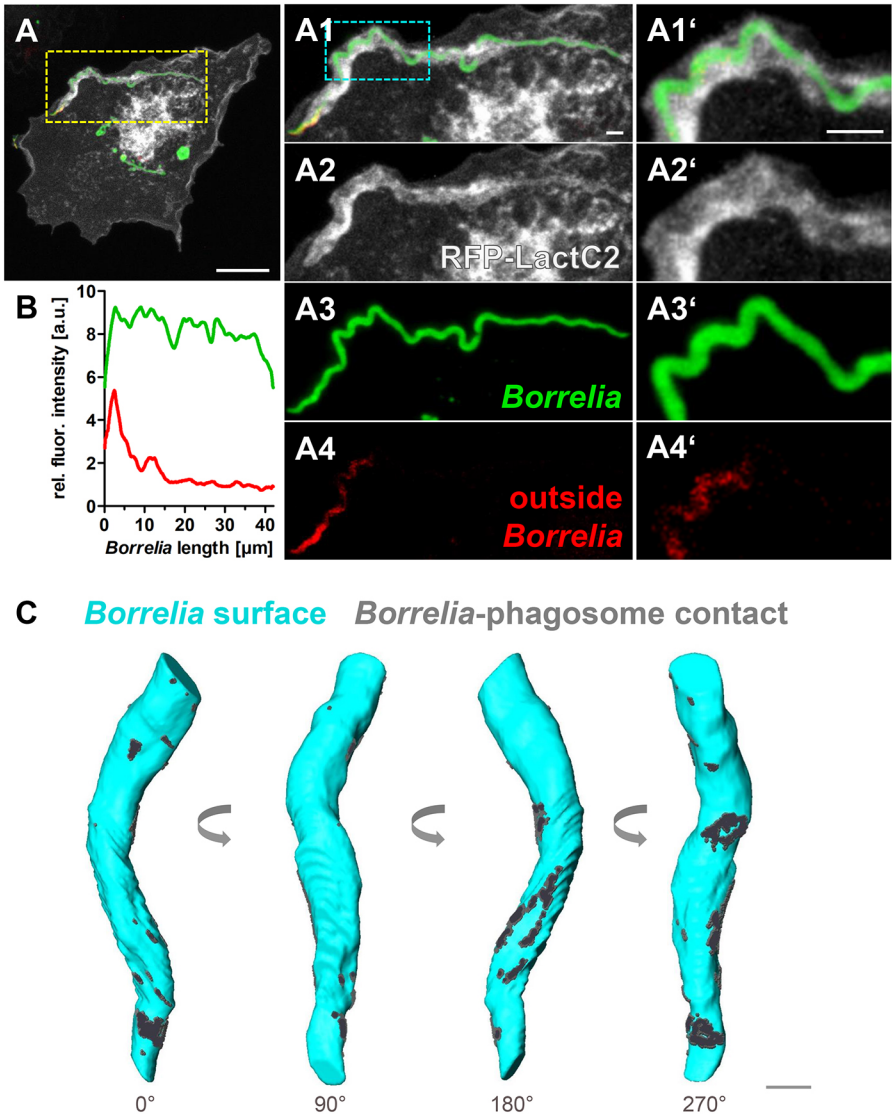

Fig. 5. *Borrelia* phagosomes have restricted access to the extracellular space. (A) Immunofluorescence micrographs of a primary macrophage expressing RFP–LactC2 (white), with internalized wild-type borreliae, stained by outside staining technique using *Borrelia*-specific antibody for antibody-accessible spirochetes (red), followed by permeabilization and staining of entire *Borrelia* cells. Yellow-dashed box in overview image A indicates region shown in detail images (A1–A4). Image representative of four observed cells from three donors. Turquoise-dashed box in detail image (A4) indicate regions shown enlarged in A1′–A4′. Note multiple points of contact between phagosomal membrane and internalized *Borrelia* cell. Also note increasingly reduced access of *Borrelia*-specific antibody to more distal parts of the phagosome, quantified and shown as line graphs (see B) for fluorescence intensities of ‘outside *Borrelia*’ (A4) and ‘*Borrelia*’ (A3) signals. Scale bars: 10 µm (A), 2 µm (A1–A4,A1′–A4′). (B) Relative fluorescence intensities and distance from start of phagosome shown in A3,A4, indicated in arbitrary units (a.u.) and µm, respectively. (C) Analysis of contact sites between the internalized *Borrelia* cell from Fig. 3 and associated phagosomal membrane using the SurfaceIntersect module of Amira™. Surface of the *Borrelia* cell shown in turquoise, contact sites between *Borrelia* cell and phagosome membrane in dark gray. Four different views rotated by each time 90° are shown. Scale bar: 0.2 µm.

Movie 7).To test whether these structures indeed represent bona fide ER contact sites, borreliae-containing phagosomes were visualized by expression of RFP–LactC2 and stained for endogenous stromal interaction molecule 1 (STIM1), a transmembrane component of ER contact sites (Balla, 2018). Indeed, multiple signals of STIM1 were found along the whole length of borreliae within RFP–LactC2-positive phagosomes (Fig. 7C,C1–C6). To visualize whether the observed STIM1 signals indeed colocalize at sites of phagosome–ER contacts, macrophages expressing mCherry–Sec61β, a marker of ER tubules (Friedman et al., 2013), were infected with GFP-expressing borreliae and also stained for endogenous STIM1. Respective immunofluorescence images showed that STIM1 signals are indeed localized at sites of contact between the ER and internalized borreliae (Fig. 7D,D1–D6,D4′–D6′,D4″–D6″). Collectively, these observations suggest that the ER forms multiple bona fide STIM1-positive contact sites with borreliae-containing phagosomes.

An updated model for phagocytosis and processing of borreliae by macrophages

Combining the findings presented here with results from previous studies (Hoffmann et al., 2014; Klose et al., 2019; Linder et al., 2001; Naj et al., 2013; Naj and Linder, 2015, 2017), we propose the following multi-step model of phagocytosis and intracellular processing of borreliae by human macrophages (Fig. 8). (1) The highly motile borreliae are immobilized at the macrophage surface through contacting filopodia. This allows sufficient time for a second actin-rich structure, the coiling pseudopod, to enwrap the spirochetes. (2) Owing to their pronounced length, captured borreliae can be partially internalized, with substantial parts of the bacteria still being outside of the host cell. Internalized borreliae are taken up into phagosomes that are positive for Rab22a and develop multiple sites of attachment with the ER. (3) Owing to the high motility of borreliae, based on the presence of endoflagellae, a subset of partially internalized bacteria can extricate themselves to a certain degree, which might also result in full escape in some cases. Extrication of borreliae leads to the formation of membrane tunnels, which probably represent sites of former phagosomes that also retain their ER contact sites. (4) Phagosomes containing internalized borreliae are compacted by the formation and abscission of membrane tubules, leading to reduction of the phagosome surface. (5) Fully compacted phagosomes follow the further pathway of phagolysosomal maturation, resulting in degradation of internalized spirochetes.

Journal of Cell Science (2021) 134, jcs252320. doi:10.1242/jcs.252320

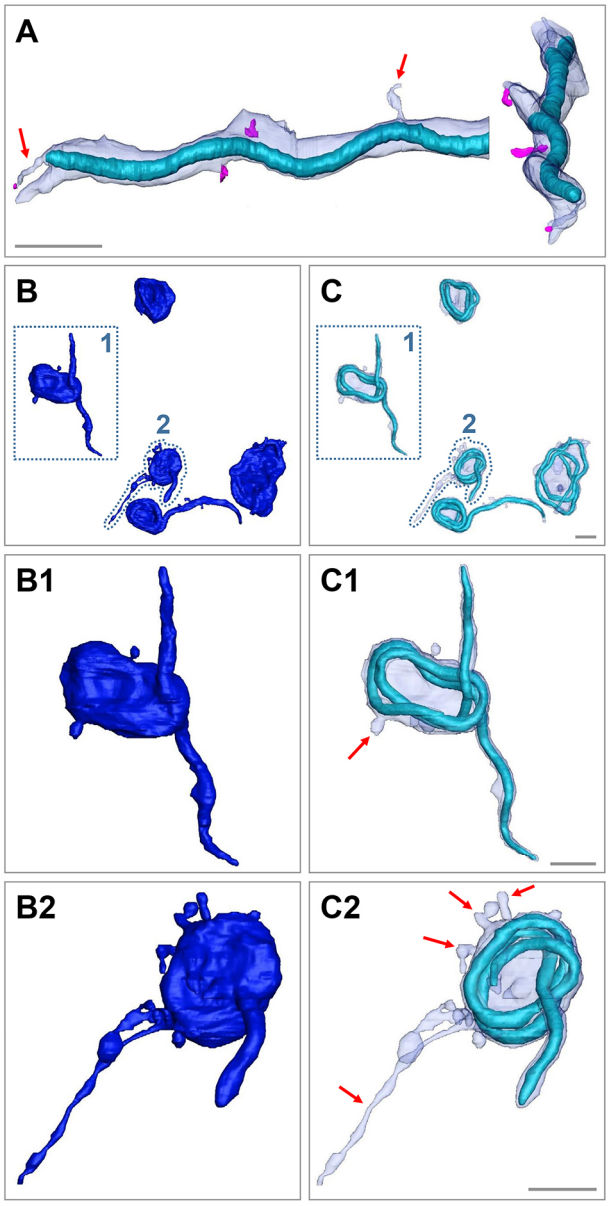

Fig. 6. Membrane tubulation at borreliae phagosomes. (A) Two perspectives of a *Borrelia* cell (magenta) internalized in a phagosome; phagosome membrane in light blue, ER contact sites in magenta. Red arrows indicate sites of membrane tubulation. Note also short membrane tunnel on the lower left. (B,C) Overviews of *Borrelia*-containing phagosomes within a single macrophage, in various stages of compaction. (B1,B2,C1,C2) individual phagsosomes enlarged from B,C. (B,B1,B2) Surface rendered in blue, and (C,C1,C2) with increased transparency. Internalized *Borrelia* cells shown in turquoise, sites of membrane tubulation indicated by red arrows. Images representative of five observed cells from three donors. Scale bars: 1 µm.

DISCUSSION

In this study, we use for the first time FIB-SEM tomography to visualize in high resolution the interaction of borreliae with primary human macrophages. We thus reveal the contribution of several membranous compartments, including phagosomes, membrane tunnels, and the ER, to intracellular processing of spirochetes. Of note, earlier ultrastructural studies of borreliae were limited by the use of conventional microscopy techniques or by focusing on specific morphological aspects of the spirochetes themselves.

A seminal study of *Borrelia* phagocytosis by human mononuclear cells showed that borreliae are engulfed in several steps by immune cells, probably due to the large size of spirochetes (Rittig et al., 1994). Moreover, borreliae were shown to be present in inclusion bodies of host cells at various stages of disintegration. (Rittig et al., 1994). However, these investigations were clearly limited by the use of single sections of cells, not allowing a spatial analysis. A further study used both light microscopy (LM) and electron microscopy (EM), but not correlative light and electron microscopy (CLEM), to investigate the interaction of borreliae with blocks of human tonsillar tissue. The study described both extracellular elongated and cystic intracellular forms of the spirochetes, without revealing further details of their interaction with host cells (Duray et al., 2005). Work by Strnad et al. actually used CLEM to investigate interaction of borreliae with mammalian neuronal cell lines. However, this was restricted to time points prior to actual uptake of spirochetes (Strnad et al., 2015).

Further ultrastructural studies of borreliae using advanced microscopy techniques focused on investigation of the spirochetes themselves. Accordingly, cryo-electron tomography was used for the analysis of chemoreceptor arrays on the *Borrelia* surface (Xu et al., 2011), or for the analysis of the cytosolic ATPase complex that associates with the flagella-specific fT3SS secretion system (Qin et al., 2018). Photo-activated localization microscopy and stochastic optical reconstruction microscopy (PALM-STORM), together with SEM, has been used to visualize the distributions of surface antigens such as OspA (Lemgruber et al., 2015), while CLEM has been applied to the analysis of the stress response of borreliae to conditions such as hypotonic media (Vancová et al., 2017).

In the current study, we used a combination of focused ion beam (FIB) and scanning electron microscopy (SEM) tomography for high-resolution analysis of borreliae interacting with human macrophages. FIB-SEM tomography enables the collection of high-resolution datasets of entire cells, which can also be precisely correlated with LM data. Of note, even using the superior combination of FIB-SEM tomography, CLEM could still be impeded by embedding cells or tissues in resin blocks, as this ensues in complicated and time-consuming relocation of target cells. This limitation can be overcome by ultra-thin embedding of cells, as performed in the current study, which allows the conservation of cell topography from LM to SEM. In classic FIB-SEM, cells are embedded in a resin block, and access to the target area has to be achieved by milling a ramp, resulting in a necessary ablation volume that is ∼10 times larger compared to that by use of ultra-thin embedding. With ultra-thin embedding, a ramp is not necessary, and only the actual volume of the region of interest is ablated (Fig. 1F), without further redeposition effects (Luckner and Wanner, 2018a,b).

Collectively, these features helped to speed up the process of FIB milling, as, for example, using ion beam currents of 50–100 nA, a macrophage of ∼50 µm diameter can be milled to its center within 5–20 min. An image stack of the corresponding region with several hundred micrographs could thus be recorded with 2 nm iso-voxels within a few hours. It is also worth noting that, during FIB-milling, the cross section of the glass slide serves as an absolute reference for precise alignment of the FIB stack. Furthermore, for FIB-SEM, the signal of the in-lens EsB detector, an energy selective backscattered electron detector placed in/above the objective lens, is standard. Therefore, we applied the in-lens SE signal from a secondary electron detector placed in/above the objective lens, as this has the additional advantages of better resolution, better signal to noise ratio and shorter exposure times (Villinger et al., 2012).

Journal of Cell Science (2021) 134, jcs252320. doi:10.1242/jcs.252320

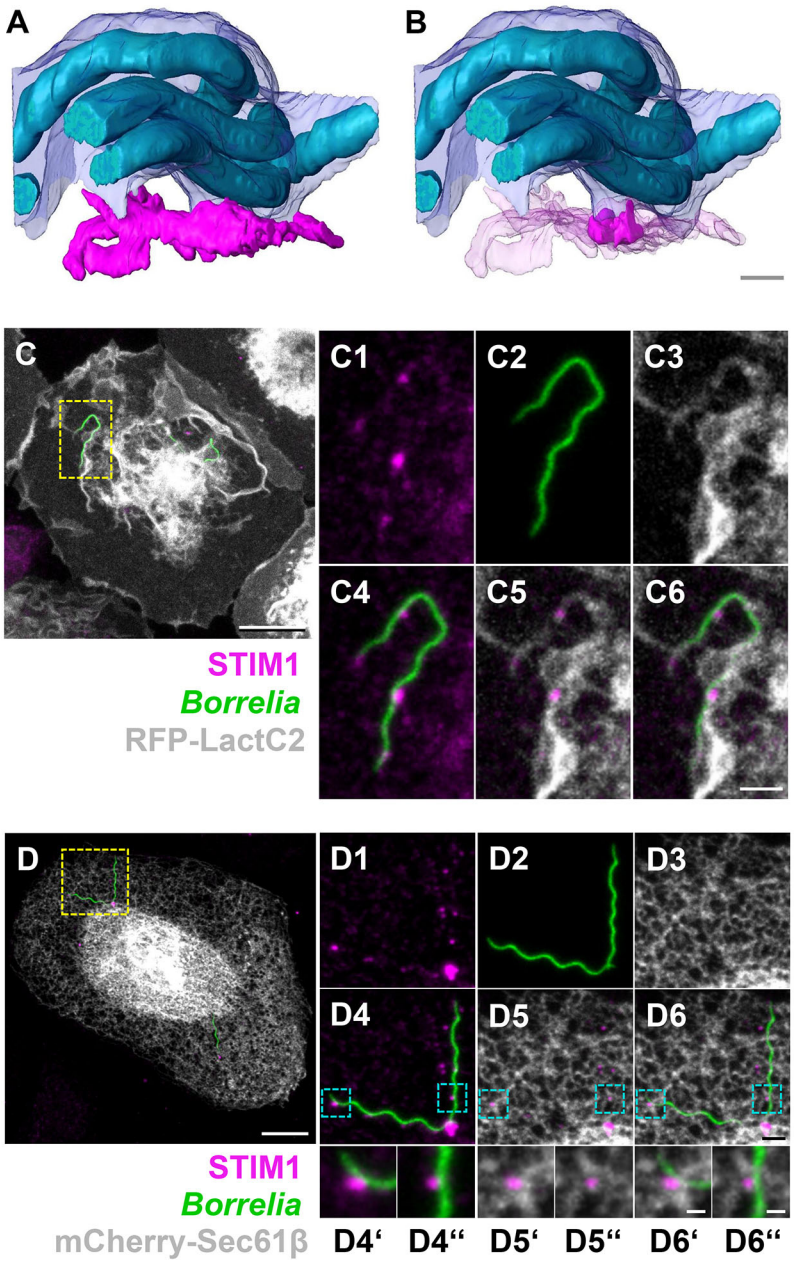

Fig. 7. Borreliae phagosomes are associated with STIM1-positive ER contact sites. (A,B) Rendering of phagosome, with phagosome surface in blue, internalized *Borrelia* cell in turquoise, and ER in magenta, with (A) showing all ER portions associated with phagosome fully colored, and (B) showing only the portions of the ER in close contact with phagosome fully colored, and the more distal parts transparent. Scale bar: 0.2 µm. (C,D) Immunofluorescence micrographs of primary macrophages expressing either RFP–LactC2 for visualization of phagosomes (C,C3) or mCherry–Sec61β for visualization of ER tubules (D,D3), incubated with GFP-expressing borreliae (C2,C2) and stained for STIM1 using specific antibody (C1,D1), with merges of two respective channels (C4,C5,D4,D5) or of all three channels (C6,D6). Yellow-dashed boxes in C,D indicate detail areas shown in C1–C6 and D1–D6; turquoise-dashed boxes in D4 indicate details areas shown in D4′–D6′ and D4″–D6″. Images representative of 15 observed cells from three donors. Scale bars: 10 µm (C,D), 2 µm (C1–C6,D1–D6), 0.5 µm (D4′–D6′, D4″–D6″).

A surprising finding from our experiments is the identification of phagosome-associated membrane tunnels. Tunnels extend from the base of internalized spirochetes into the cytoplasm of the host cell and are thus larger than the actual phagosomes. We hypothesized that tunnel formation could be due to partial extrication of the highly motile borreliae from macrophages. To study this in more detail, we used RFP–LactC2 as a reporter for phosphatidylserine (Kay and Grinstein, 2011; Yeung et al., 2008), a modified phosphoglycerol present at the inner leaflet of the plasma membrane. Phosphatidylserine is thus also part of the outer membrane of endosomes and phagosomes that are derived from plasma membrane material (Maxson and Grinstein, 2020). Indeed, we could observe that borreliae-containing phagosomes were also positive for RFP–LactC2. Moreover, in ∼2–5% of all partial internalizations, RFP–LactC2 signals extended >5 µm further into the cytoplasm than the internalized parts of spirochetes themselves. These uptake events were associated with large parts of the *Borrelia* cells still being outside of the host cell. It is thus highly likely that RFP–LactC2-positive phagosome extensions correspond to the membrane tunnels identified by FIB-SEM, and also that membrane tunnels are formed as a result of partial extrication of borreliae, based on their flagella-powered motility.

An obvious question concerns the potential content of membrane tunnels. Use of an antibody-based outside staining technique showed that incompletely closed phagosomes retain access to the extracellular space. However, at least for antibodies, this access is progressively restricted towards the distal end of the phagosome. This probably reflects the gradual accumulation of contact sites between enclosed spirochetes and the phagosome membrane along the length of the phagosome, which can be observed both in immunofluorescence image and also using software-based surface contact reconstruction (Fig. 5). Larger molecules, such as antibodies, may thus no longer be able to diffuse freely within the whole phagosomes. However, smaller solutes or the extracellular

Journal of Cell Science (2021) 134, jcs252320. doi:10.1242/jcs.252320

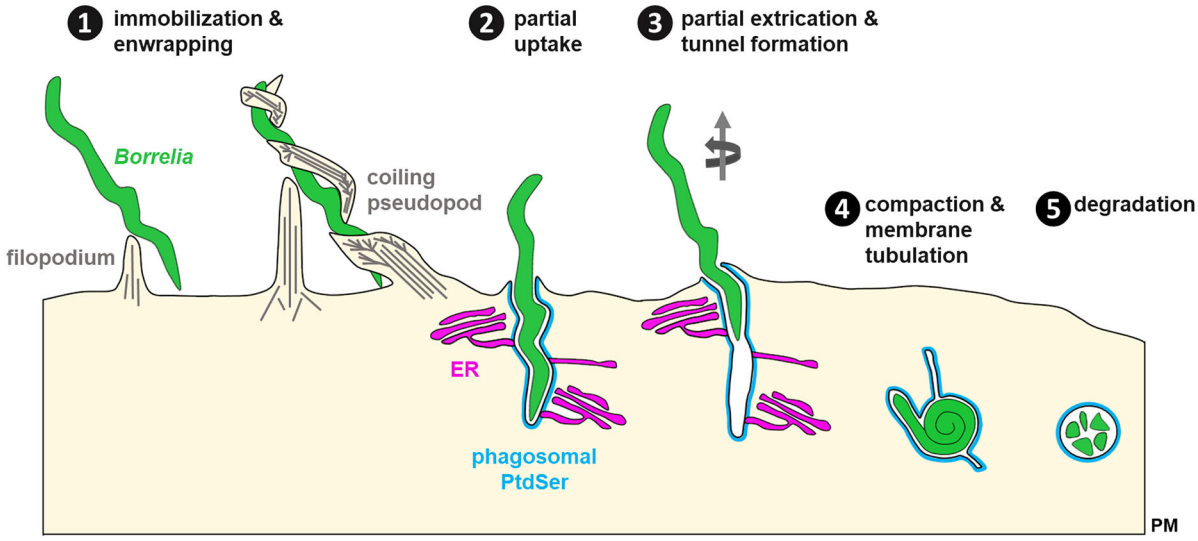

Fig. 8. Model of *Borrelia* uptake and intracellular processing by macrophages. (1) Highly motile spirochets are immobilized by contact with filopodia of the host cell, followed by enwrapment by a coiling pseudopod. (2) Contraction of the pseudopod leads to partial uptake of the *Borrelia* cell and formation of a nascent phagosome positive for phosphatidylserine (PtdSer) that is contacted by the ER. Note that only phagosomal PtdSer, not plasma membrane-associated one, is shown. (3) Endoflagella-based motility of the extracellular portion of the *Borrelia* cell can lead to partial extrication of the spirochete and formation of an intracellular membrane tunnel which retains contact to the ER. (4) Formation of membrane tubules leads to reduction of the phagosome surface and compaction of spirochetes, followed by (5) degradation in mature phagolysosomes. PM, plasma membrane; PtdSer: phosphatidylserine.

medium may still have access to the whole phagosome volume. This concept would also be in line with earlier observations that, in fixed specimens, some borreliae-containing phagosomes could be completely stained by Ruthenium Red, indicating continuity of these structures with the extracellular space (Rittig et al., 1994). Apart from the resulting restrictions of access for larger molecules, there is currently no indication that these contacts between spirochetes and the phagosomal membrane are of special significance during the phagosomal process. They appear to be more a consequence of size restrictions within and compaction of phagosomes. It should be noted that incompletely closed phagosomes do not necessarily follow the outline of highly bent spirochetes closely (Fig. 5), probably allowing some intraphagosomal movement of borreliae, indicating that intra-phagosomal contacts between borreliae and the phagosomal membrane are not permanent. Moreover, formation of tunnels, likely based on partial extrication of spirochetes, also points to a transient nature of these areas of contact.

The fact that membrane tunnels have not been described so far is probably due to several reasons: (1) that they are only formed in a subset of uptake events, where partially internalized borreliae are able to extricate themselves from the host cell to a certain degree; (2) previous analyses of borreliae–host cell interaction were mostly based on a limited number of EM sections, with a specific spatial orientation, while FIB-SEM used here allows for the first time analysis of the complete three-dimensional space surrounding the nascent phagosomes; and (3) tunnel formation is likely based on strong active propulsion by partially internalized *Borrelia*. It will thus be especially interesting to investigate whether the formation of membrane tunnels is a general phenomenon that also applies to the uptake of other highly motile and elongated bacteria such as *Legionella* or *Treponema* by phagocytes.

Previously, we have shown that internalization of borreliae by macrophages involves compaction of spirochetes into more globular forms. This is apparently achieved by membrane tubules being formed and detached from phagosomes, thus progressively reducing the phagosomal surface (Naj and Linder, 2015). Nevertheless, formation of membrane tubules is difficult to visualize in live-cell imaging, as such events take place in a matter of minutes and also proceed in multiple optical planes. The frequency of these events thus remained an open question. The FIB-SEM analysis used here confirms and extends our previous observations and indicates that membrane tubulation at phagosomes is indeed a frequent phenomenon which likely contributes to phagolysosomal compaction of spirochetes, which is a prerequisite for their further intracellular processing.

Interestingly, formation of membrane tubules is apparently initiated at sites of contact between Rab5a-positive endosomes with the Rab22a-positive phagosomal coat (Naj and Linder, 2015). These endosomes are also positive for SNX3, a sorting nexin containing a phospholipid-binding Phox domain, which enables vesicle docking to regions of the phagosomal surface that are enriched in the phosphoinositide PI(3)P (Klose et al., 2019). This phenomenon is most likely due to the enhanced activity of phosphoinositide 3-kinase (PI3K) at sites of membrane curvature discontinuities (Hubner et al., 1998). Such membrane bends are frequently formed at borreliae phagosomes due to the helical shape of the bacteria. Of note, the SNX3 C-terminus, a region of 11 amino acid residues that binds galectin-9, has been shown to be crucial for phagosomal compaction (Klose et al., 2019). Binding of the SNX3 and Rab5a double-positive vesicles thus leads to recruitment of galectin-9 vesicles. Using single and combinatorial knockdowns, we have previously shown that galectin-9 acts in the same pathway as SNX3. Moreover, both carbohydrate-binding domains of galectin-9 are required for its role in borreliae phagosome tubulation. However, use of point mutations showed that none of the currently known residues involved in binding specific carbohydrates, such as Ala46 for binding of Forssman pentasaccharides (Nagae et al., 2008) or Arg221 for sialylated oligosaccharides (Yoshida et al., 2010), are important for phagosomal tubulation (Klose et al., 2019). The

molecular mechanism by which galectin-9 regulates borreliae phagosomal compaction is thus currently unresolved.

In contrast to the C-terminus of SNX3, its N-terminus, which recruits retromer complex (Lucas et al., 2016), does not influence membrane tubulation and phagosomal compaction (Klose et al., 2019), indicating that SNX3 and Rab5a double-positive vesicles likely function independently of retromer in the process of borreliae phagosome compaction. Our observations here that membrane tubulation is a frequent event at borreliae-containing phagosomes, and thus probably decisive for their compaction, indicates that retromer-independent processes might also occur at other phagosomes, in particular those containing spirochetes such as *Legionella* or *Treponema*.

Furthermore, the FIB-SEM-based reconstructions presented here show that the ER closely associates with all borreliae-containing membranous structures. This includes both nascent phagosomes and phagosomes undergoing compaction, but also membrane tunnels. The latter probably reflects the ER contact sites being retained during partial extrication and relocation of borreliae within nascent phagosomes. Considering that tunnels are most probably caused by extrication of borreliae, and membrane tubules are formed by active extrusion of material from the phagosome surface, both structures can be distinguished by their diameters and relative location at phagosomes. As former sites of borreliae phagosomes, tunnels have a diameter that roughly corresponds to the diameter of borreliae (~0.5 µm), even in case of potential shrinkage. Moreover, tunnels are by definition only formed at the distal end of partially phagocytosed borreliae. By contrast, membrane tubules at phagosomes show smaller diameters (~0.2 µm) and can be formed all over the surface of borreliae phagosomes (see Fig. 6), which can also be observed in live cell imaging (Naj and Linder, 2015).

Importantly, the observation that the ER forms numerous contact sites with borreliae-containing phagosomes is in line with our earlier findings of a close spatial correlation between both structures in live-cell imaging, with the ER often enwrapping nascent phagosomes (Naj and Linder, 2015). Indeed, it had been shown earlier that endosomes form close contacts with the ER and that they maintain these contact sites during their maturation from early Rab5-positive to late Rab7-positive vesicles (Friedman et al., 2013; Phillips and Voeltz, 2016).

Along similar lines, it has become evident that the ER is closely associated with both nascent and maturing phagosomes. This is reflected by the formation of multiple specialized contact sites between the ER and phagosomes (Levin-Konigsberg and Grinstein, 2020; Nunes et al., 2012). ER–phagosome contact sites have been proposed to fulfill multiple, so far speculative, functions, including localized transfer of phosphatidylinositols or of Ca^{2+} ions, or to act as coordinating sites for membrane tubulation and fission events (Levin-Konigsberg and Grinstein, 2020). The latter would be in analogy to the proven function of the ER as a marker for sites of tubulation and fission of endosomes (Rowland et al., 2014).

However, it is currently unclear whether this scenario is also true for phagosomes. Still, the findings that phagolysosome resolution (1) requires contact with the ER, for transfer of PI(4)P to the ER by the Rab7 effector ORP1L, and (2) is accompanied by membrane tubulation and fission events (Levin-Konigsberg et al., 2019), indicate that the ER could also support membrane tubulation and fission at phagosomes. Moreover, in the current study, we could show that STIM1 localizes to contacts between the ER and borreliae phagosomes, indicating that these locations represent bona fide ER contact sites. STIM1 is an ER-resident transmembrane protein that activates store-operated Ca^{2+} channels, and has, so far, been detected at phagosomes containing zymosan particles (Nunes et al., 2012), sheep red blood cells (Guido et al., 2015) or *Chlamydia trachomatis* (Agaisse and Derre, 2015). *Borrelia burgdorferi* is thus only the second bacterium whose phagosomal uptake has been associated with recruitment of STIM1 and formation of ER contact sites. Considering that localized Ca^{2+} entry has been shown to regulate phagosomal NADPH oxidase activity (Dewitt et al., 2003) and phagosome–lysosome fusion (Jaconi et al., 1990), this also points to a central role of ER–phagosome contacts and STIM1-regulated Ca^{2+} levels in the maturation of *Borrelia*-containing phagosomes, and likely in the intracellular processing of other pathogenic and non-pathogenic bacteria as well.

Collectively, the analyses presented here confirm and extend the knowledge on architecture, composition and function of membranous host cell compartments during uptake and intracellular processing of borreliae by human immune cells. They also indicate that the actual uptake process might be more complex than previously believed, with its ultimate outcome depending on partial internalization and partial extrication of borreliae within a complex tug-of-war between spirochetes and human immune cells.

MATERIALS AND METHODS

Isolation and culturing of macrophages

Primary human macrophages were isolated as monocytes from the leukocyte fraction of buffy coats (kindly provided by Frank Bentzien, UKE Transfusion Medicine, Hamburg, Germany) as described previously (Naj et al., 2013). Monocytes were isolated from buffy coats by sucrose density gradient centrifugation in Ficoll (PromoCell, Heidelberg, Germany); 20 ml blood was coated on 15 ml Ficoll and centrifuged for 30 min at 4°C and 460 ***g*** (without fast acceleration and brake). Leukocyte fractions were transferred into a new 50 ml tube and filled up to 50 ml with cold RPMI 1640 medium (Invitrogen, Carlsbad, USA). Cells were washed twice in cold RPMI 1640 and centrifuged for 10 min at 4°C and 460 ***g***. Enriched leukocytes were resuspended in 1.5 ml sterile monocyte buffer [2 mM EDTA and 0.5% human serum albumin in Dulbecco's PBS (DPBS), pH 7.4], mixed with 250 µl of a suspension of magnetic beads coupled to CD14 antibodies (Miltenyi Biotec, Bergisch Gladbach, Germany) and incubated for 15 min on ice. The mixture was then loaded on a MS^{+} Separation column (Miltenyi Biotec, Bergisch Gladbach, Germany) previously placed in a magnetic holder and equilibrated with 1 ml cold monocyte buffer. Trapped $CD14^{+}$ monocytes were washed twice on column with 1 ml monocyte buffer and, after the removal of the magnet, were eluted with 3 ml monocyte buffer into 15 ml cold RPMI 1640. Cells were seeded on six-well plates (Sarstedt, Nürnbrecht, Germany) at a density of 2×10^{6} cells per well and diluted with cold RPMI 1640 for this. After adhesion of monocytes, RPMI medium was replaced by 1.5 ml monocyte culture medium [RPMI 1640 supplemented with 20% autologous human serum (prepared in-house), 100 U/ml penicillin and 100 µg/ml streptavidin]. Monocytes were cultivated in an incubator at 37°C, 5% CO_2 and 90% humidity and differentiated into macrophages. After 6 days, the culture medium was replaced by fresh monocyte culture medium. Differentiation into macrophages was routinely checked by expression of marker proteins such as CD68, high phagocytic capacity, cell size (>20 µm diameter) and typical radially symmetric morphology under non-stimulating conditions, as well as restructuring of the actin cytoskeleton, including the formation of >100 podosomes per cell (Cervero et al., 2013).

Borrelia culture

Wild-type *Borrelia burgdorferi* strain B31 (kindly provided by Peter Kraiczy, Department of Medical Microbiology and Hospital Hygiene, Goethe-Universität, Frankfurt/Main, Germany) and GFP-expressing *B. burgdorferi* B31 5A4 NP1 strain (Moriarty et al., 2008) (kindly provided by George Chaconas, Department of Biochemistry and Molecular Biology, University of Calgary, Canada) were cultivated in complete BSK-H (Sigma-Aldrich, Taufkirchen, Germany) or BSK-II medium prepared in-house (Barbour,

1984) containing 6% normal rabbit serum. Genetically modified borreliae were kept under antibiotic selection pressure using 100 µg/ml gentamicin and 200 µg/ml kanamycin. Liquid bacterial cultures were cultivated under microaerophilic conditions at 33°C and ∼1% CO_2.

Borrelia microscopy

For determination of cell number, morphology and motility, 10 µl of (diluted) *Borrelia* cultures were filled in a disposable C-Chip Neubauer improved hemocytometer (Digital Bio, Seoul, South Korea) and analyzed by dark field microscopy using a Nikon Eclipse Ci-L upright microscope equipped with LED illuminator, Nikon CFI Achromat 10× NA0.25/7.00, CFI Achromat 20× LWD/NA0.40/3.90 and CFI Achromat 40× NA0.65/0.65 objective lenses, and two Nikon CFI 10×/22 mm oculars (Nikon Microscope Solutions, Düsseldorf, Germany).

Preparation of *Borrelia*-infected macrophage samples for FIB-SEM

At 7 days after isolation and differentiation, primary human macrophages were seeded in monocyte culture medium at a total number of 32,000 cells on glass object slides with laser-etched grids. Cells were infected with GFP-expressing borreliae at an MOI 30:1 in RPMI 1640 at 37°C for 1 h and subsequently fixed in 2% methanol-free formaldehyde supplemented with 0.5% glutaraldehyde (both EM-grade, Thermo Fisher Scientific, Karlsruhe, Germany). Slides/coverslips were rinsed with PBS (Thermo Fisher Scientific, Karlsruhe, Germany) and immediately fixed with 2.5% glutaraldehyde (Science Services GmbH, Munich, Germany) in 75 mM cacodylate (Sigma-Aldrich, Taufkirchen, Germany), 75 mM NaCl, 2 mM $MgCl_2$ for 30 min, followed by three washing steps in cacodylate buffer.

Light microscopy of infected macrophages

Cells were stained with DAPI, and sealed with a coverslip and Fixogum (Marabu GmbH & Co. KG, Tamm, Germany) to prevent drying during light microscopy investigation. ROIs were marked on a template, with the same coordinates. For documentation, two of three different magnifications (objectives 5×, 10× and 40×) were sufficient to retrieve ROIs in SEM. Depending on specimen properties, bright field, phase contrast or DIC was used. For correlative CLSM of infected macrophages, overview images were acquired in 'tile scan' mode to select cells in the desired stage. Emission of GFP and DAPI was collected using standard filter sets for GFP (486–564 nm) and DAPI (403–473 nm). Confocal *z*-stacks (113.27×113.27×15.86 µm) were recorded with an image pixel size of 78 nm in *xy* and 260 nm in *z*.

Cell transfection and phagocytosis assays

Transient transfection of primary human macrophages with plasmid DNA was performed using the Neon transfection system (Life Technologies, Carlsbad, USA) with settings: pulse voltage, 1000 V; pulse width, 40 ms; and pulse number, 2. Cells were transfected at a ratio of 10^5 cells to 0.5 µg of GFP–Rab22a plasmid DNA (a kind gift from Julie Donaldson, Cell Biology and Physiology Center, National Heart, Lung, and Blood Institute, National Institutes of Health, Bethesda, MD, USA) and 1 µg of RFP–LactC2pDNA (a kind gift from Sergio Grinstein, Hospital for Sick Children, University of Toronto, ON, Canada) or mCherry–Sec61β (a kind gift from Gia Voeltz, Department of Molecular, Cellular, and Developmental Biology, University of Colorado-Boulder, Boulder, CO, USA) in R-buffer. Transfected macrophages were infected with wild-type borreliae at a MOI 100:1 or with GFP-expressing borreliae at a MOI 15:1 in RPMI 1640 at 37°C for 30 min prior to fixation and immunofluorescence staining.

Immunofluorescence staining and confocal microscopy

Transfected macrophages were seeded at a density of 10^5 cells per glass coverslip (12-mm diameter) and fixed for 10 min in 4% methanol-free formaldehyde to avoid permeabilization, washed three times in PBS, and blocked with 2% BSA for 30 min. Cells were incubated with rabbit primary polyclonal antibody against *Borrelia burgdorferi* (Antibodies Online, ABIN236885; 1:1000) in blocking solution for 60 min. After three washes with PBS, cells were incubated for 30 min with anti-rabbit-IgG secondary antibody coupled to Alexa Fluor 405 (Thermo Fisher Scientific, Carlsbad, USA; 1:200) in PBS for outside staining. For staining of entire wild-type *Borrelia* cells, macrophages were permeabilized with 0.1% Triton X-100 in PBS for 10 min and again incubated with blocking solution and primary antibodies as performed for outside staining. Cells were incubated with anti-rabbit-IgG Alexa Fluor 647 secondary antibodies afterwards for 30 min (Thermo Fisher Scientific, Carlsbad, USA; 1:200) and intensively washed with PBS prior to mounting. STIM1 was stained by rabbit primary monoclonal antibody (Cell Signaling, #5668S, 1:500) and secondary anti-rabbit-IgG Alexa Fluor 647 antibody (1:200). Coverslips were mounted on glass slides with Mowiol 4-88 (Roth, Karlsruhe, Germany) containing p-phenylenediamine (Sigma-Aldrich, Taufkirchen, Germany). Images of fixed samples were acquired with confocal laser-scanning microscope Leica DMi8 (with a TCS SP8 AOBS confocal point scanner) equipped with an oil-immersion 63× HC PL APO Oil CS2 NA 1.40 objective and Leica LAS X SP8 software (Leica Microsystems, Wetzlar, Germany). Quantification of diminishing antibody staining (Fig. 5C) was performed using ImageJ 1.52p and GraphPad Prism 5.04. Using the immunofluorescence micrograph showing antibody staining against the whole *Borrelia* cell, a segmented line was drawn along the helical shape of the entire bacterium, resulting in an intensity plot profile in ImageJ. The same segmented line was used to plot an intensity profile in the micrograph showing the outside *Borrelia* staining. Resulting intensity data were smoothed with GraphPad Prism using LOWESS smoothing.

Electron microscopy sample preparation

After removal of Fixogum and coverslips, cells were post-fixed with 1% OsO_4 and 1% $K_4Fe(CN)_6$ in cacodylate buffer for 30 min, washed three times in ddH_2O, incubated with 1% thiocarbohydrazide in ddH_2O for 30 min, washed with ddH_2O three times, followed by post-fixation with 1% OsO_4 in ddH_2O for 30 min. The samples were rinsed three times with ddH_2O and dehydrated in a graded series of acetone (10%, 20%, 40%, 60%, 80% and 100%), containing a 1% uranyl acetate step in 20% acetone for 30 min, infiltrated and embedded on the glass slide.

Ultra-thin embedding and conductive coating

Cells were infiltrated with 1:1 Hard-Plus Resin-812 in acetone for 15 min, 2:1 (resin:acetone) for 30 min and 3:1 (resin:acetone) for 30 min. A filter paper, completely soaked with acetone, was placed at the bottom of a Falcon® tube to provide an acetone-saturated atmosphere. A polypropylene cap was placed on top of the filter paper to avoid direct contact with the slide. The slide was placed upright into the Falcon® tube for 10–30 min, allowing excessive resin to drain into the filter paper at the bottom of the Falcon® tube. The samples were polymerized for 72 h at 60°C. Glass slides were reduced to the appropriate size by fracturing with aid of a diamond pen. The specimens were mounted on aluminum stubs with colloidal silver and coated with a carbon layer of 15 nm by evaporation.

FIB-SEM tomography

Infected macrophages were imaged in an Auriga 40 FIB-SEM workstation operating under SmartSEM® (Carl Zeiss Microscopy GmbH, Oberkochen, Germany) or Atlas 3D (Fibics incorporated, Ottawa, Canada). FIB-SEM milling was started right in front of the cell. Ion beam currents (dependent on the stability of the resin) of 50 pA to 10 nA were used. Depending on the desired resolution, image pixel sizes between 2 nm and 10 nm in *x*/*y* were chosen. For large volume analysis, milling rate was set to 3 or 5 nm. Owing to metallic ferrocyanide-reduced osmium-thiocarbohydrazide-ferrocyanide-reduced osmium (rOTO) impregnation of the cells, conducting the slides with colloidal silver and carbon coating of the specimens, charging was completely avoided. The rOTO impregnation provides a strong material contrast; therefore, shorter exposure times down to 17 s/image (3072×2048 pixel) could be achieved.

3D Rendering

The datasets were aligned using Amira™ (Thermo Fisher Scientific, Carlsbad, USA) with the module 'align slices'. The image stacks, either from CLSM or FIB-SEM, were segmented and reconstructed in Amira™ or processed with a direct volume rendering algorithm (volren) for immediate visualization.

Acknowledgements
We thank Frank Bentzien for buffy coats, George Chaconas for GFP-expressing *B. burgdorferi* B31 5A4 NP1, Julie Donaldson for GFP–Rab22a, Sergio Grinstein for RFP–LactC2, Peter Kraiczy for wild-type *B. burgdorferi* B31, Gia Voeltz for mCherry–Sec61β, Andrea Mordhorst for expert technical assistance, the UKE microscope facility (umif) for help with microscopy and image analysis, and Martin Aepfelbacher for continuous support.

Competing interests
The authors declare no competing or financial interests.

Author contributions
Conceptualization: M.K., G.W., S.L.; Methodology: M.K., M.L., G.W., S.L.; Software: M.S.; Validation: G.W., S.L.; Formal analysis: M.S., M.L.; Investigation: M.K., M.L., G.W.; Resources: S.L.; Data curation: M.K., M.S., G.W., S.L.; Writing - original draft: S.L.; Writing - review & editing: G.W., S.L.; Visualization: M.K., M.S., G.W., S.L.; Supervision: G.W., S.L.; Project administration: G.W., S.L.; Funding acquisition: M.K., S.L.

Funding
This work has been supported by a research stipend from University Clinic Hamburg-Eppendorf (to M.K.), and a grant from Deutsche Forschungsgemeinschaft (GRK1459, to S.L.).

Supplementary information
Supplementary information available online at
https://jcs.biologists.org/lookup/doi/10.1242/jcs.252320.supplemental

Peer review history
The peer review history is available online at
https://jcs.biologists.org/lookup/doi/10.1242/jcs.252320.reviewer-comments.pdf

References

Aberer, E. and Duray, P. H. (1991). Morphology of Borrelia burgdorferi: structural patterns of cultured borreliae in relation to staining methods. *J. Clin. Microbiol.* **29**, 764-772. doi:10.1128/JCM.29.4.764-772.1991

Agaisse, H. and Derre, I. (2015). STIM1 is a novel component of ER-chlamydia trachomatis inclusion membrane contact sites. *PLoS ONE* **10**, e0125671. doi:10.1371/journal.pone.0125671

Balla, T. (2018). Ca(2+) and lipid signals hold hands at endoplasmic reticulum-plasma membrane contact sites. *J. Physiol.* **596**, 2709-2716. doi:10.1113/JP274957

Barbour, A. G. (1984). Isolation and cultivation of lyme-disease spirochetes. *Yale J. Biol. Med.* **57**, 521-525.

Benach, J. L., Fleit, H. B., Habicht, G. S., Coleman, J. L., Bosler, E. M. and Lane, B. P. (1984). Interactions of phagocytes with the Lyme disease spirochete: role of the Fc receptor. *J. Infect. Dis.* **150**, 497-507. doi:10.1093/infdis/150.4.497

Carreras-Gonzalez, A., Barriales, D., Palacios, A., Montesinos-Robledo, M., Navasa, N., Azkargorta, M., Pena-Cearra, A., Tomas-Cortazar, J., Escobes, I., Pascual-Itoiz, M. A. et al. (2019). Regulation of macrophage activity by surface receptors contained within Borrelia burgdorferi-enriched phagosomal fractions. *PLoS Pathog.* **15**, e1008163. doi:10.1371/journal.ppat.1008163

Cervero, P., Panzer, L. and Linder, S. (2013). Podosome reformation in macrophages: assays and analysis. *Methods Mol. Biol.* **1046**, 97-121. doi:10.1007/978-1-62703-538-5_6

Chang, Y., Moon, K. H., Zhao, X., Norris, S. J., Motaleb, M. A. and Liu, J. (2019). Structural insights into flagellar stator-rotor interactions. *eLife* **8**, e48979. doi:10.7554/eLife.48979.031

Cinco, M., Murgia, R., Presani, G. and Perticarari, S. (1997). Integrin CR3 mediates the binding of nonspecifically opsonized Borrelia burgdorferi to human phagocytes and mammalian cells. *Infect. Immun.* **65**, 4784-4789. doi:10.1128/IAI.65.11.4784-4789.1997

Dewitt, S., Laffafian, I. and Hallett, M. B. (2003). Phagosomal oxidative activity during beta2 integrin (CR3)-mediated phagocytosis by neutrophils is triggered by a non-restricted Ca2+ signal: Ca2+ controls time not space. *J. Cell Sci.* **116**, 2857-2865. doi:10.1242/jcs.00499

Duray, P. H., Yin, S. R., Ito, Y., Bezrukov, L., Cox, C., Cho, M. S., Fitzgerald, W., Dorward, D., Zimmerberg, J. and Margolis, L. (2005). Invasion of human tissue ex vivo by Borrelia burgdorferi. *J. Infect. Dis.* **191**, 1747-1754. doi:10.1086/429632

Friedman, J. R., Dibenedetto, J. R., West, M., Rowland, A. A. and Voeltz, G. K. (2013). Endoplasmic reticulum-endosome contact increases as endosomes traffic and mature. *Mol. Biol. Cell* **24**, 1030-1040. doi:10.1091/mbc.e12-10-0733

Goldstein, S. F., Charon, N. W. and Kreiling, J. A. (1994). Borrelia burgdorferi swims with a planar waveform similar to that of eukaryotic flagella. *Proc. Natl. Acad. Sci. USA* **91**, 3433-3437. doi:10.1073/pnas.91.8.3433

Guido, D., Demaurex, N. and Nunes, P. (2015). Junctate boosts phagocytosis by recruiting endoplasmic reticulum Ca2+ stores near phagosomes. *J. Cell Sci.* **128**, 4074-4082. doi:10.1242/jcs.172510

Hawley, K. L., Olson, C. M., Jr, Iglesias-Pedraz, J. M., Navasa, N., Cervantes, J. L., Caimano, M. J., Izadi, H., Ingalls, R. R., Pal, U., Salazar, J. C. et al. (2012). CD14 cooperates with complement receptor 3 to mediate MyD88-independent phagocytosis of Borrelia burgdorferi. *Proc. Natl. Acad. Sci. USA* **109**, 1228-1232. doi:10.1073/pnas.1112078109

Hoffmann, A. K., Naj, X. and Linder, S. (2014). Daam1 is a regulator of filopodia formation and phagocytic uptake of Borrelia burgdorferi by primary human macrophages. *FASEB J.* **28**, 3075-3089. doi:10.1096/fj.13-247049

Hubner, S., Couvillon, A. D., Kas, J. A., Bankaitis, V. A., Vegners, R., Carpenter, C. L. and Janmey, P. A. (1998). Enhancement of phosphoinositide 3-kinase (PI 3-kinase) activity by membrane curvature and inositol-phospholipid-binding peptides. *Eur. J. Biochem.* **258**, 846-853. doi:10.1046/j.1432-1327.1998.2580846.x

Jaconi, M. E., Lew, D. P., Carpentier, J. L., Magnusson, K. E., Sjogren, M. and Stendahl, O. (1990). Cytosolic free calcium elevation mediates the phagosome-lysosome fusion during phagocytosis in human neutrophils. *J. Cell Biol.* **110**, 1555-1564. doi:10.1083/jcb.110.5.1555

Kay, J. G. and Grinstein, S. (2011). Sensing phosphatidylserine in cellular membranes. *Sensors (Basel)* **11**, 1744-1755. doi:10.3390/s110201744

Klose, M., Salloum, J. E., Gonschior, H. and Linder, S. (2019). SNX3 drives maturation of Borrelia phagosomes by forming a hub for PI(3)P, Rab5a, and galectin-9. *J. Cell Biol.* **218**, 3039-3059. doi:10.1083/jcb.201812106

Kudryashev, M., Cyrklaff, M., Alex, B., Lemgruber, L., Baumeister, W., Wallich, R. and Frischknecht, F. (2011). Evidence of direct cell-cell fusion in Borrelia by cryogenic electron tomography. *Cell. Microbiol.* **13**, 731-741. doi:10.1111/j.1462-5822.2011.01571.x

Lane, R. S. and Loye, J. E. (1991). Lyme disease in California: interrelationship of ixodid ticks (Acari), rodents, and Borrelia burgdorferi. *J. Med. Entomol.* **28**, 719-725. doi:10.1093/jmedent/28.5.719

Lemgruber, L., Sant'Anna, C., Griffths, C., Abud, Y., Mhlanga, M., Wallich, R. and Frischknecht, F. (2015). Nanoscopic localization of surface-exposed antigens of borrelia burgdorferi. *Microsc. Microanal.* **21**, 680-688. doi:10.1017/S1431927615000318

Levin-Konigsberg, R. and Grinstein, S. (2020). Phagosome-endoplasmic reticulum contacts: kissing and not running. *Traffic* **21**, 172-180. doi:10.1111/tra.12708

Levin-Konigsberg, R., Montano-Rendon, F., Keren-Kaplan, T., Li, R., Ego, B., Mylvaganam, S., DiCiccio, J. E., Trimble, W. S., Bassik, M. C., Bonifacino, J. S. et al. (2019). Phagolysosome resolution requires contacts with the endoplasmic reticulum and phosphatidylinositol-4-phosphate signalling. *Nat. Cell Biol.* **21**, 1234-1247. doi:10.1038/s41556-019-0394-2

Li, C., Motaleb, A., Sal, M., Goldstein, S. F. and Charon, N. W. (2000). Spirochete periplasmic flagella and motility. *J. Mol. Microbiol. Biotechnol.* **2**, 345-354.

Linder, S., Heimerl, C., Fingerle, V., Aepfelbacher, M. and Wilske, B. (2001). Coiling phagocytosis of Borrelia burgdorferi by primary human macrophages is controlled by CDC42Hs and Rac1 and involves recruitment of Wiskott-Aldrich syndrome protein and Arp2/3 complex. *Infect. Immun.* **69**, 1739-1746. doi:10.1128/IAI.69.3.1739-1746.2001

Liu, J., Lin, T., Botkin, D. J., McCrum, E., Winkler, H. and Norris, S. J. (2009). Intact flagellar motor of Borrelia burgdorferi revealed by cryo-electron tomography: evidence for stator ring curvature and rotor/C-ring assembly flexion. *J. Bacteriol.* **191**, 5026-5036. doi:10.1128/JB.00340-09

Lucas, M., Gershlick, D. C., Vidaurrazaga, A., Rojas, A. L., Bonifacino, J. S. and Hierro, A. (2016). Structural mechanism for cargo recognition by the retromer complex. *Cell* **167**, 1623-1635.e1614. doi:10.1016/j.cell.2016.10.056

Luckner, M. and Wanner, G. (2018a). From light microscopy to analytical scanning electron microscopy (SEM) and focused ion beam (FIB)/SEM in biology: fixed coordinates, flat embedding, absolute references. *Microsc. Microanal.* **24**, 526-544. doi:10.1017/S1431927618015015

Luckner, M. and Wanner, G. (2018b). Precise and economic FIB/SEM for CLEM: with 2 nm voxels through mitosis. *Histochem. Cell Biol.* **150**, 149-170. doi:10.1007/s00418-018-1681-x

Maxson, M. E. and Grinstein, S. (2020). The role of membrane surface charge in phagocytosis. *Adv. Exp. Med. Biol.* **1246**, 43-54. doi:10.1007/978-3-030-40406-2_3

Montgomery, R. R., Nathanson, M. H. and Malawista, S. E. (1994). Fc- and non-Fc-mediated phagocytosis of Borrelia burgdorferi by macrophages. *J. Infect. Dis.* **170**, 890-893. doi:10.1093/infdis/170.4.890

Moriarty, T. J., Norman, M. U., Colarusso, P., Bankhead, T., Kubes, P. and Chaconas, G. (2008). Real-time high resolution 3D imaging of the lyme disease spirochete adhering to and escaping from the vasculature of a living host. *PLoS Pathog.* **4**, e1000090. doi:10.1371/journal.ppat.1000090

Nagae, M., Nishi, N., Nakamura-Tsuruta, S., Hirabayashi, J., Wakatsuki, S. and Kato, R. (2008). Structural analysis of the human galectin-9 N-terminal carbohydrate recognition domain reveals unexpected properties that differ from the mouse orthologue. *J. Mol. Biol.* **375**, 119-135. doi:10.1016/j.jmb.2007.09.060

Naj, X. and Linder, S. (2015). ER-Coordinated activities of Rab22a and Rab5a drive phagosomal compaction and intracellular processing of borrelia burgdorferi by macrophages. *Cell Reports* **12**, 1816-1830. doi:10.1016/j.celrep.2015.08.027

Naj, X. and Linder, S. (2017). Actin-dependent regulation of borrelia burgdorferi phagocytosis by macrophages. *Curr. Top. Microbiol. Immunol.* **399**, 133-154. doi:10.1007/82_2016_26

Naj, X., Hoffmann, A. K., Himmel, M. and Linder, S. (2013). The formins FMNL1 and mDia1 regulate coiling phagocytosis of Borrelia burgdorferi by primary human macrophages. *Infect. Immun.* **81**, 1683-1695. doi:10.1128/IAI.01411-12

Nunes, P., Cornut, D., Bochet, V., Hasler, U., Oh-Hora, M., Waldburger, J. M. and Demaurex, N. (2012). STIM1 juxtaposes ER to phagosomes, generating Ca(2)(+) hotspots that boost phagocytosis. *Curr. Biol.* **22**, 1990-1997. doi:10.1016/j.cub.2012.08.049

Phillips, M. J. and Voeltz, G. K. (2016). Structure and function of ER membrane contact sites with other organelles. *Nat. Rev. Mol. Cell Biol.* **17**, 69-82. doi:10.1038/nrm.2015.8

Qin, Z., Tu, J., Lin, T., Norris, S. J., Li, C., Motaleb, M. A. and Liu, J. (2018). Cryo-electron tomography of periplasmic flagella in Borrelia burgdorferi reveals a distinct cytoplasmic ATPase complex. *PLoS Biol.* **16**, e3000050. doi:10.1371/journal.pbio.3000050

Rittig, M. G., Krause, A., Haupl, T., Schaible, U. E., Modolell, M., Kramer, M. D., Lutjen-Drecoll, E., Simon, M. M. and Burmester, G. R. (1992). Coiling phagocytosis is the preferential phagocytic mechanism for Borrelia burgdorferi. *Infect. Immun.* **60**, 4205-4212. doi:10.1128/IAI.60.10.4205-4212.1992

Rittig, M. G., Haupl, T., Krause, A., Kressel, M., Groscurth, P. and Burmester, G. R. (1994). Borrelia burgdorferi-induced ultrastructural alterations in human phagocytes: a clue to pathogenicity? *J. Pathol.* **173**, 269-282. doi:10.1002/path.1711730311

Rowland, A. A., Chitwood, P. J., Phillips, M. J. and Voeltz, G. K. (2014). ER contact sites define the position and timing of endosome fission. *Cell* **159**, 1027-1041. doi:10.1016/j.cell.2014.10.023

Salazar, J. C., Pope, C. D., Sellati, T. J., Feder, H. M., Jr, Kiely, T. G., Dardick, K. R., Buckman, R. L., Moore, M. W., Caimano, M. J., Pope, J. G. et al. (2003). Coevolution of markers of innate and adaptive immunity in skin and peripheral blood of patients with erythema migrans. *J. Immunol.* **171**, 2660-2670. doi:10.4049/jimmunol.171.5.2660

Strnad, M., Elsterová, J., Schrenková, J., Vancová, M., Rego, R. O., Grubhoffer, L. and Nebesářová, J. (2015). Correlative cryo-fluorescence and cryo-scanning electron microscopy as a straightforward tool to study host-pathogen interactions. *Sci. Rep.* **5**, 18029. doi:10.1038/srep18029

Svitkina, T. M., Bulanova, E. A., Chaga, O. Y., Vignjevic, D. M., Kojima, S., Vasiliev, J. M. and Borisy, G. G. (2003). Mechanism of filopodia initiation by reorganization of a dendritic network. *J. Cell Biol.* **160**, 409-421. doi:10.1083/jcb.200210174

Vancová, M., Rudenko, N., Vaněček, J., Golovchenko, M., Strnad, M., Rego, R. O. M., Ticha, L., Grubhoffer, L. and Nebesářová, J. (2017). Pleomorphism and viability of the lyme disease pathogen borrelia burgdorferi exposed to physiological stress conditions: a correlative Cryo-fluorescence and Cryo-scanning electron microscopy study. *Front. Microbiol.* **8**, 596. doi:10.3389/fmicb.2017.00596

Villinger, C., Gregorius, H., Kranz, C., Höhn, K., Münzberg, C., von Wichert, G., Mizaikoff, B., Wanner, G. and Walther, P. (2012). FIB/SEM tomography with TEM-like resolution for 3D imaging of high-pressure frozen cells. *Histochem. Cell Biol.* **138**, 549-556. doi:10.1007/s00418-012-1020-6

Xu, H., Raddi, G., Liu, J., Charon, N. W. and Li, C. (2011). Chemoreceptors and flagellar motors are subterminally located in close proximity at the two cell poles in spirochetes. *J. Bacteriol.* **193**, 2652-2656. doi:10.1128/JB.01530-10

Yeung, T., Gilbert, G. E., Shi, J., Silvius, J., Kapus, A. and Grinstein, S. (2008). Membrane phosphatidylserine regulates surface charge and protein localization. *Science* **319**, 210-213. doi:10.1126/science.1152066

Yoshida, H., Teraoka, M., Nishi, N., Nakakita, S., Nakamura, T., Hirashima, M. and Kamitori, S. (2010). X-ray structures of human galectin-9 C-terminal domain in complexes with a biantennary oligosaccharide and sialyllactose. *J. Biol. Chem.* **285**, 36969-36976. doi:10.1074/jbc.M110.163402